

# Impacts of Hardware Impairments on Mutualistic Cooperative Ambient Backscatter Communications

Yinghui Ye, Liqin Shi, Xiaoli Chu, Guangyue Lu, and Sumei Sun

## Abstract

In mutualistic cooperative ambient backscatter communications (AmBC), Internet-of-Things (IoT) device sends its information to a desired receiver by modulating and backscattering the primary signal, while providing beneficial multipath diversity to the primary receiver in return, thus forming a mutualism relationship between the AmBC and primary links. We note that the hardware impairments (HIs), which are unavoidable in practical systems and may significantly affect the transmission rates of the primary and AmBC links and their mutualism relationships, have been largely ignored in the study of mutualistic cooperative AmBC networks. In this paper, we consider a mutualistic cooperative AmBC network under HIs, and study the impacts of HIs on the achievable rates of the primary link and the AmBC link. In particular, we theoretically prove that although HIs degrades the rate of each link, the mutualism relationship between the AmBC and primary links is maintained, i.e., the rate of the primary link in the mutualistic cooperative AmBC network is still higher than that without the AmBC link. The closed-form

This work was supported in part by the the Natural Science Basic Research Program of Shaanxi under Grant 2021JQ-713, in part by the Young Talent fund of University Association for Science and Technology in Shaanxi under Grant 20210121, in part by the Scientific Research Program Funded by Shaanxi Provincial Education Department under Grant 21JK0914.

Yinghui Ye, Liqin Shi and Guangyue are with the Shaanxi Key Laboratory of Information Communication Network and Security, Xi'an University of Posts & Telecommunications, China. (connectyuh@126.com, liqinshi@hotmail.com, tonylugy@163.com)

Xiaoli Chu is with the Department of Electronic and Electrical Engineering, The University of Sheffield, U.K. (e-mail: x.chu@sheffield.ac.uk)

Sumei Sun is with the Institute of Infocomm Research, Agency for Science, Technology and Research, Singapore. (e-mail: sunsm@i2r.a-star.edu.sg)

rate expressions of both the AmBC and primary links are derived. Computer simulations are provided to validate our theoretical analysis.

### **Index Terms**

Ambient backscatter communications, hardware impairment, mutualism relationship.

## I. INTRODUCTION

Ambient backscatter communications (AmBC) have been proposed as a spectrum- and energy- efficient solution for Internet of Things (IoT) [1], [2]. The basic principle of AmBC is to allow an IoT device adjusting the antenna's load impedance to passively modulate information on the primary signals and backscatter the modulated signals to the associated receiver so that the power-hungry components can be avoided in IoT devices [2], [3]. AmBC was validated by various practical prototypes [4]–[6]. In AmBC, the AmBC receiver receives signals from both the primary transmitter (PT) and the AmBC transmitter<sup>1</sup> simultaneously, and the PT's signal, e.g., cellular signal, is usually much stronger than that of AmBC. Meanwhile, due to the non-cooperative spectrum sharing between the primary and AmBC link, it is hard for the AmBC receiver to obtain the channel state information of each link, and hence cannot remove the severe co-channel interferences caused by the PT's signal [7]. Accordingly, the transmission performance of AmBC links is limited and may not meet the requirement of IoT devices. Cooperative AmBC [8], where the primary link and the AmBC link are jointly designed, has appeared as a promising solution to overcome the above challenge. Depending on whether the AmBC modulation rate is equal to or much slower than that of PT, cooperative AmBC is classified into parasitic cooperative AmBC and mutualistic cooperative AmBC. In the former, the AmBC receiver firstly decodes the PT's signal while treating the interference from the AmBC link as noise and then removes the decoded PT signal from the composite received signal to decode the AmBC signal [9]. In the latter, as the AmBC modulation rate is much slower than that of the PT and the received AmBC signal includes both the PT's and IoT device's information,

<sup>1</sup>In this paper, the AmBC transmitter and the IoT device are interchangeably used.

the AmBC link provides an additional multipath gain for the primary receiver to decode PT's signal, forming a mutualism relationship between the primary and AmBC links [8].

In [10], the authors maximized the weighted sum rate of both the primary and AmBC links by jointly optimizing the PT's transmit power and beamforming vectors in parasitic and mutualistic cooperative AmBC networks, respectively. The similar optimizations were also studied in [11] by considering the finite block length in AmBC links. The authors of [12] formulated a stochastic optimization to maximize the utility function of the signal-to-interference-plus-noise ratio (SINR) in a parasitic cooperative AmBC network. Considering the energy-causality constraint at each IoT device, the authors in [13] jointly optimized the PT's transmit power and the IoT device's power reflection coefficient and backscattering time to maximize the energy efficiency in parasitic and mutualistic cooperative AmBC networks, respectively. In addition to the above works [10]–[13] with a focus on resource allocation, the performance evaluation was also investigated in cooperative AmBC networks. In [14], the outage probability and the diversity gain for a parasitic cooperative AmBC network were derived. Combining parasitic cooperative AmBC with downlink non-orthogonal multiple access (NOMA), the outage probability and ergodic capacity were analyzed theoretically in [15]. Considering a mutualistic cooperative AmBC network, the authors in [16] derived the upper bounds of the ergodic capacity for both the primary and AmBC links.

In the above works [10]–[16], the radio frequency (RF) front ends of each transceiver are assumed to be ideal, which may be unrealistic. This is because in practical communications, RF front ends are susceptible to a variety of hardware impairments (HIs), e.g., in-phase/quadrature imbalance, quantization error, etc, distorting signals generated by the transmitter and thus degrading the information decoding performance at the receiver [17]. In spite of the efforts on the development of mitigation algorithms, there always exist residual HIs due to the time-varying hardware characteristics. Accordingly, HIs should be taken into consideration in the study of cooperative AmBC networks. However, to the best of our knowledge, only in a very recent work [18], the authors derived the expressions for both the outage probability and intercept probability in a *parasitic* cooperative NOMA-AmBC network, where the RF front ends of all

transceivers suffer HIs. That is, the impacts of HIs on the *mutualistic* cooperative AmBC network are still unknown. In particular, when the HIs exist, the AmBC link not only brings the additional multipath but also backscatters the distortion noises that are generated by the PT's front ends to the primary link. More specifically, if allowing an IoT device to share spectrum with a primary link via AmBC does not benefit the primary link's rate, then there is no return for the primary link and no mutualism relationship. In this regard, a natural question arises: *Does the mutualism relationship between the primary and AmBC links still exist in the presence of HIs?*

In this work, we consider a *mutualistic* cooperative AmBC network under HIs, where the IoT device modulates its information on the PT's signal with a much slower modulation rate compared with that of the PT. Our goal is to reveal the impacts of HIs and answer the above question. The main contributions are summarized as follows.

We theoretically prove the following three results that achieve the above goal. First, the primary link's rate under HIs is strictly smaller than that under ideal hardware. Second, for given HI parameters, the primary link's rate that is derived when the AmBC link exists is strictly larger than that without any AmBC link. The above two results validate that the existence of HIs degrades the rate of both the AmBC and primary links but does not destroy the mutualism relationship between the AmBC and primary links. Compared with [10], our conclusion<sup>2</sup> is more rigorous and the details are summarized in Remark 2. Third, we demonstrate that the HIs lead to the rate ceilings for the primary and AmBC links by deriving the upper-bound rates of the primary link and that of the AmBC link at a very high PT's transmit power. Besides, under the assumption that the modulated information of the IoT device follows a symmetric complex Gaussian distribution, we derive closed-form rate expressions of both the primary and AmBC links.

<sup>2</sup>The ideal hardware in [10] is a special case of our considered model, thus the conclusion that mutualism relationship between the AmBC and primary links exists is also valid for the ideal case.

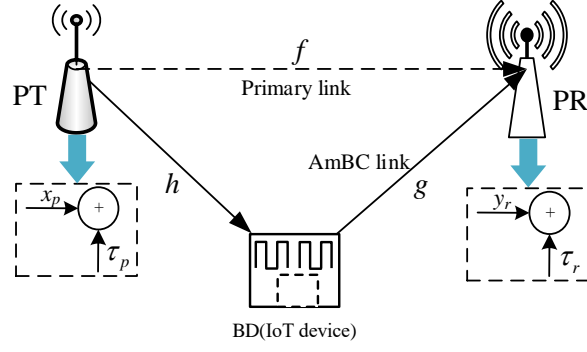


Fig. 1. System model.

## II. SYSTEM MODEL AND RATE ANALYSIS

Fig. 1 is a mutualistic cooperative AmBC network that consists of one primary transmitter (PT), one primary receiver (PR), and one IoT device (also referred to as a backscatter device (BD) in this paper). Both PT and PR are non-energy-constrained transceivers that are composed of active components, e.g., oscillators. Denote  $h$ ,  $f$ ,  $g$  as the channel gains of the PT-BD link, the PT-PR link (also termed as the primary link), and the BD-PR link (also termed as the AmBC link), respectively. A block-fading channel model is considered, i.e., all the channel gains stay constant within each transmission block but may change across different transmission blocks. To obtain the performance bound of both primary and AmBC links, we assume perfect channel state information.

Let  $x_p(n)$  and  $c_s(i)$  denote the primary signal in the  $n$ -th symbol period and the AmBC signal in the  $i$ -th symbol period, respectively. Due to the simple backscatter circuit in the BD and the low modulation rate of the BD, the symbol period of  $x_p(n)$ , denoted by  $T_p$ , is shorter than that of  $c_s(i)$ , denoted by  $T_c$ . For analytical tractability, we assume that  $T_c = LT_p$ , where  $L \gg 1$  is a positive integer, and that  $x_p(n)$  follows an independent circularly symmetric complex Gaussian distribution, i.e.,  $x_p(n) \sim \mathcal{CN}(0, 1)$ . Also, the mean and variance of  $c_s(i)$  are assumed to be zero and one, respectively.

In the considered network, PT and BD work in the cooperative mode and transmit their information to the PR by sharing the same resource block. More specifically, PT conveys information to the PR, meanwhile, BD modulates its own information on the PT's signals and reflects the modulated signal to

the PR. Accordingly, the transmit signal of the PT and the received signal of the BD can be written as, respectively<sup>3</sup>,

$$y_{\text{PT}}(n) = x_p(n) + \tau_p(n), \quad (1)$$

$$y_{\text{BD}}(n) = \sqrt{h}(x_p(n) + \tau_p(n)), \quad (2)$$

where  $\tau_p(n)$  is the distortion noise caused by HIs of the PT.  $\tau_p(n)$  follows an independent zero-mean circularly symmetric complex Gaussian distribution, and its variance is the product of the average power of the PT's signal  $P_0$  and the HIs level parameter  $\kappa_p$  [17], i.e.,  $\tau_p(n) \sim \mathcal{CN}(0, \kappa_p^2 P_0)$ .

Accordingly, the received signal of the PR is expressed as

$$y_{\text{PR}}(n) = \underbrace{\sqrt{\beta h g}(x_p(n) + \tau_p(n)) c_s(i)}_{\text{PT} \rightarrow \text{BD} \rightarrow \text{PR link}} + \underbrace{\sqrt{f}(x_p(n) + \tau_p(n))}_{\text{PT} \rightarrow \text{PR link}} + \tau_r(n) + w(n), \quad (3)$$

where  $w(n)$  is the additive complex white Gaussian noise with mean zero and variance  $\sigma^2$ ,  $\beta$  is the power reflection coefficient,  $\tau_r(n)$  is the hardware distortion noise introduced by the PR with the HIs level parameter  $\kappa_r$ . The power of  $\tau_r(n)$ , for given  $|c_s(i)|^2$ , equals  $\kappa_r^2 P_0 (1 + \kappa_p^2) (h\beta g |c_s(i)|^2 + f)$ , while for each transmission block, the power of  $\tau_r(n)$  can be calculated as  $\kappa_r^2 P_0 (1 + \kappa_p^2) (h\beta g \mathbb{E}[|c_s(i)|^2] + f) = \kappa_r^2 P_0 (1 + \kappa_p^2) (h\beta g + f)$ . Accordingly, the distribution of  $\tau_r(n)$  can be written as

$$\tau_r(n) \sim \begin{cases} \mathcal{CN}(0, \kappa_r^2 P_0 (1 + \kappa_p^2) (h\beta g |c_s(i)|^2 + f)), & \text{within one BD's symbol} \\ \mathcal{CN}(0, \kappa_r^2 P_0 (1 + \kappa_p^2) (h\beta g + f)), & \text{within one transmission block} \end{cases} \quad (4)$$

Due to  $T_c = LT_p$ ,  $c_s(i)$  spans  $L$  primary symbol periods for  $n = 1, 2, \dots, L$ , i.e.,  $c_s(i)$  keeps almost unchanged for decoding  $x_p(n)$ ,  $n = 1, 2, \dots, L$ . For a given  $c_s(i)$ , the first term in (3) can be rewritten as  $\sqrt{\beta h g} x_p(n) c_s(i) + \sqrt{\beta h g} \tau_p(n) c_s(i)$ , where  $\sqrt{\beta h g} x_p(n) c_s(i)$  and  $\sqrt{\beta h g} \tau_p(n) c_s(i)$  can be regarded as the output of the PT signal  $x_p(n)$  passing through a slowly varying channel  $\sqrt{\beta h g} c_s(i)$  and the Gaussian noise

<sup>3</sup>Similar to [7], [8], here we omit the thermal noise at the BD as its power introduced by the passive components is much smaller than that of  $h(x_p(n) + \tau_p(n))$ .

with variance  $\kappa_p^2 P_0 \beta h g |c_s(i)|^2$ , respectively. Accordingly, the SINR to decode  $x_p(n)$  and the achievable rate of  $x_p(n)$  within the symbol period of  $c_s(i)$  can be calculated as, respectively,

$$\gamma_{x_p}(c_s(i)) = \frac{P_0 h \beta g |c_s(i)|^2 + P_0 f}{P_0 (h \beta g |c_s(i)|^2 + f) \kappa + \sigma^2}, \quad (5)$$

$$R_p(c_s(i)) = B_w \log_2 (1 + \gamma_{x_p}(c_s(i))), \quad (6)$$

where  $\kappa = \kappa_r^2 \kappa_p^2 + \kappa_r^2 + \kappa_p^2$ , and  $B_w$  denotes the communication bandwidth.

Assuming that the number of symbols of the BD signal is sufficiently large within one transmission block, then the average rate of  $x_p(n)$  is given as

$$\mathcal{C}_p = \mathbb{E}_{c_s(i)} [R_p(c_s(i))], \quad (7)$$

where  $\mathbb{E}_x[\cdot]$  denotes the expectation operator over the random variable  $x$ .

After obtaining the rate of the primary link, we put our attention on the rate of the AmBC link. As one of main focuses in this work is to see whether the existence of HIs destroys the mutualism transmission in the mutualistic cooperative AmBC network or not, we assume for simplicity that  $\sqrt{hf}x_p(n)$  can be perfectly removed from  $y_{\text{PR}}(n)$  via successive interference cancellation (SIC). Thus, the remaining signal at the PR to decode  $c_s(i)$  is given by

$$\begin{aligned} \hat{y}_{\text{PR}}(n) &= \sqrt{\beta h g} (x_p(n) + \tau_p(n)) c_s(i) \\ &+ \sqrt{f} \tau_p(n) + \tau_r(n) + w(n). \end{aligned} \quad (8)$$

As the average power of  $x_p(n)$  equals one and one BD symbol  $c_s(i)$  is modulated into the  $L$  consecutive PT symbol periods  $x_p(n)$ , the average SINR to decode  $c_s(i)$  via maximal ratio combining (MRC) of  $\hat{y}_{\text{PR}}(n)$ ,  $n = 1, 2, \dots, L$ , which are received in  $L$  consecutive primary symbol periods, in each transmission block, can be approximated as

$$\gamma_{c_s} = \sum_{n=1}^L \mathbb{E} \left[ \frac{\beta h g |x_p(n)|^2}{|\tau_p(n)|^2 (\beta h g + f) + |\tau_r(n)|^2 + |w(n)|^2} \right] = \frac{L \beta h g P_0}{P_0 (\beta h g + f) \kappa + \sigma^2}. \quad (9)$$

In the mutualistic cooperative AmBC network, as modulating one BD symbol requires  $L$  consecutive PT symbols, the PT's signal  $x_p(n)$  can be viewed as a spread-spectrum code with length  $L$  for BD symbols.

Accordingly, the SINR to decode  $c_s(i)$  is increased by  $L$  times at the price of symbol rate decreased by  $\frac{1}{L}$ , and the BD's rate can be expressed as

$$\mathcal{C}_s = \frac{B_w}{L} \log_2 (1 + \gamma_{c_s}). \quad (10)$$

### III. IMPACTS OF HIS ON RATE

The rates for the primary link and the AmBC link with ideal hardware can be obtained by substituting  $\kappa_p = \kappa_r = 0$  into (7) and (10), respectively, given as

$$\mathcal{C}_p^{\text{id}} = \mathbb{E}_{c_s(i)} \left[ B_w \log_2 \left( 1 + \frac{P_0 h \beta g |c_s(i)|^2 + P_0 f}{\sigma^2} \right) \right], \quad (11)$$

$$\mathcal{C}_s^{\text{id}} = \frac{B_w}{L} \log_2 \left( 1 + \frac{L P_0 \beta h g}{\sigma^2} \right). \quad (12)$$

Comparing the rates in (11) and (12) with the HIs case in (7) and (10), it is clear that the rates with HIs are strictly smaller than those of ideal hardware, i.e.,  $\mathcal{C}_p^{\text{id}} > \mathcal{C}_p$  and  $\mathcal{R}_s^{\text{id}} > \mathcal{R}_s$  always hold when  $\kappa > 0$ . This indicates that the existence of HIs degrades the achievable rates of both the primary and AmBC links. Besides, by assuming  $P_0 \rightarrow \infty$  in the case of HIs, we have the following inequality associated with the PT's rate, i.e.,

$$\begin{aligned} \mathcal{C}_p &\leq B_w \log_2 \left( 1 + \frac{h \beta g \mathbb{E} [|c_s(i)|^2] + f}{(h \beta g \mathbb{E} [|c_s(i)|^2] + f) \kappa + \frac{\sigma^2}{P_0}} \right) \\ &< B_w \log_2 \left( 1 + \frac{1}{\kappa} \right), \end{aligned} \quad (13)$$

where the first inequality holds for the Jensen's inequality, and second inequality is derived from that  $\frac{h \beta g \mathbb{E} [|c_s(i)|^2] + f}{(h \beta g \mathbb{E} [|c_s(i)|^2] + f) \kappa + \frac{\sigma^2}{P_0}}$  is an increasing function with respect to  $P_0$  and that  $\frac{\sigma^2}{P_0}$  approaches to zero as  $P_0 \rightarrow \infty$ .

Similar as above, we can obtain the following inequality on the BD's rate as  $P_0 \rightarrow \infty$ , given by

$$\mathcal{C}_s < \frac{B_w}{L} \log_2 \left( 1 + \frac{L \beta h g}{(\beta h g + f) \kappa} \right) \quad (14)$$

*Remark 1.* Both (13) and (14) show that the HIs level parameter have significant impacts on the achievable rate. It can be seen that in the case of HIs, the achievable rates of both the primary and

AmBC links are bounded at  $P_0 \rightarrow \infty$ , i.e., there exist rate ceilings for both the primary and AmBC links. Interestingly, the upper bound of  $C_p$  *only* depends on the HIs level parameter, while for the AmBC link, its upper bound is affected by the HIs level parameter and the channel gains. Particularly, the upper bound of  $C_s$  increases with the decrease of  $f$ , indicating that a poor channel condition of the PT-PR link raises the ceiling of the AmBC link rate.

We note that in this seminal contribution [10], it has been shown that in the ideal hardware case, allowing BD to share the same spectrum with the PT can offer multipath diversity to the primary link without introducing any harmful factors and thus the primary link achieves a larger transmission rate than the case where the spectrum resource is alone used by the PT, yielding the mutualism transmission between primary and AmBC links. However, in the presence of HIs, the AmBC link not only provides beneficial multipath to the primary link, but also brings the extra hardware distortion noise that is a harmful factor to the primary link's rate. In this regard, a natural question arises: does the mutual benefit still hold in the presence of HIs? To answer this question, we provide the following theorem.

**Theorem 1.** For given  $\kappa$  and all channel gains, we have the following inequality, i.e.,

$$C_p > B_w \log_2 \left( 1 + \frac{P_0 f}{P_0 f \kappa + \sigma^2} \right), \quad (15)$$

where the right side of (15) is the achievable rate when the spectrum resource is alone used by the PT, i.e., access denied for BD, in the case of HIs.

*Proof.* Please refer to Appendix A. ■

*Remark 2.* Theorem 1 indicates that in the mutualistic cooperative AmBC network with HIs, even though the access of BDs brings both multipath diversity and hardware distortion noise to the primary link, the rate of the primary link can be still improved. That is, the existence of HIs does not destroy the mutual benefit between the AmBC and primary links. In particular, letting  $\kappa_p = \kappa_r = 0$  ( $\kappa = \kappa_r^2 \kappa_p^2 + \kappa_r^2 + \kappa_p^2 = 0$ ), Theorem 1 also verifies that the mutual benefit exists in the ideal hardware case. We note that the existence of mutual benefit in the ideal hardware case was also proven in [10], where the assumption that  $c_s(i)$  follows the complex Gaussian distribution and the approximation under high signal-noise-ratio (SNR)

were adopted, however, in our work, we have not made any special assumptions on the distribution of  $c_s(i)$  and also have not used any approximations. Thus, our proposed Theorem 1 is more general and rigorous compared to the existing one [10].

Although we provide expressions to calculate  $\mathcal{C}_p$  and its upper bound, (7) is not in the closed form and (13) is tight only at  $P_0 \rightarrow \infty$ . This indicates that the upper bound in (13) does not hold at low or moderate transmit power. Accordingly, it is required to derive a closed-form expression that approximates  $\mathcal{C}_p$  well no matter what the transmit power is. To this end, Proposition 1 is provided.

**Proposition 1.** By assuming that  $c_s(i)$  follows the symmetric complex Gaussian distribution with zero mean and unit variance, we can approximate  $\mathcal{C}_p$  as

$$\mathcal{C}_p = \begin{cases} B_w \log_2 \left( \frac{b+b\kappa+\sigma^2}{b\kappa+\sigma^2} \right) - \frac{B_w}{\ln 2} \exp \left( \frac{b+b\kappa+\sigma^2}{a\kappa+a} \right) \text{Ei} \left( -\frac{b+b\kappa+\sigma^2}{a\kappa+a} \right) \\ + \frac{B_w}{\ln 2} \exp \left( \frac{b\kappa+\sigma^2}{a\kappa} \right) \text{Ei} \left( -\frac{b\kappa+\sigma^2}{a\kappa} \right), \text{ if } \kappa > 0 \\ B_w \log_2 \left( \frac{b+\sigma^2}{\sigma^2} \right) - \frac{B_w}{\ln 2} \exp \left( \frac{b+\sigma^2}{a} \right) \text{Ei} \left( -\frac{b+\sigma^2}{a} \right), \text{ if } \kappa = 0 \end{cases}, \quad (16)$$

where  $a = P_0 h \beta g$ ,  $b = P_0 f$ , and  $\text{Ei}(\cdot)$  is the exponential integral.

*Proof.* Please refer to Appendix B. ■

*Remark 3.* By comparisons between (16) and the right side of (15), one can see that the increased rates of the primary link in the case of HIs and ideal hardware case are  $\frac{B_w}{\ln 2} \exp \left( \frac{b\kappa+\sigma^2}{a\kappa} \right) \text{Ei} \left( -\frac{b\kappa+\sigma^2}{a\kappa} \right) - \frac{B_w}{\ln 2} \exp \left( \frac{b+b\kappa+\sigma^2}{a\kappa+a} \right) \text{Ei} \left( -\frac{b+b\kappa+\sigma^2}{a\kappa+a} \right)$  and  $-\frac{B_w}{\ln 2} \exp \left( \frac{b+\sigma^2}{a} \right) \text{Ei} \left( -\frac{b+\sigma^2}{a} \right)$ , respectively. It can be inferred that the HIs degrade the increased rate, as  $-\frac{B_w}{\ln 2} \exp \left( \frac{b+\sigma^2}{a} \right) \text{Ei} \left( -\frac{b+\sigma^2}{a} \right) > \frac{B_w}{\ln 2} \exp \left( \frac{b\kappa+\sigma^2}{a\kappa} \right) \text{Ei} \left( -\frac{b\kappa+\sigma^2}{a\kappa} \right) - \frac{B_w}{\ln 2} \text{Ei} \left( -\frac{b+b\kappa+\sigma^2}{a\kappa+a} \right) \exp \left( \frac{b+b\kappa+\sigma^2}{a\kappa+a} \right)$  holds at  $\kappa > 0$ . This indicates that although the existence of HIs does not destroy the mutual benefit between the primary and AmBC links, the harmful impacts on the increased rate exist.

#### IV. SIMULATIONS

In this section, computer simulations are provided to support our findings. Unless otherwise specified, the basic simulation parameters are set as follows. In particular, we set  $P_0 = 3$  mW,  $T = 1$  s,  $B_w = 1$  MHz,  $L = 128$ ,  $\kappa_p = \kappa_r = 0.1$ , and the noise power spectral density is set as  $\sigma^2 = -120$  dBm/Hz [10],

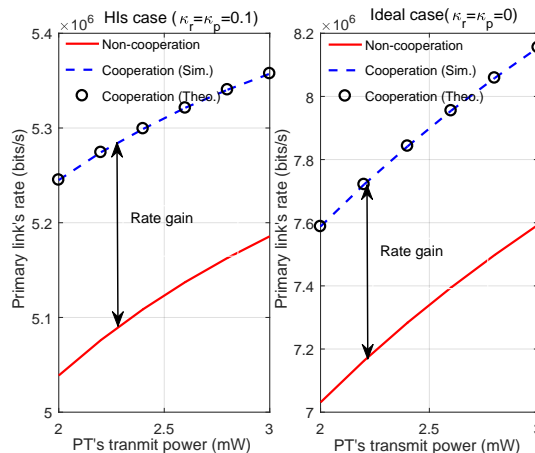


Fig. 2. The PT's rate versus the transmit power of the PT  $P_0$  under the HIs case and the ideal case.

[18]. The standard channel fading model is considered, where each channel gain is given by the product of the small-scale fading and the large-scale fading. Let  $D_{ps}$ ,  $D_{sr}$  and  $D_{pr}$  denote the distances of the PT-BD link, the BD-PR link and the PT-PR link, respectively. Denote  $h'$ ,  $f'$  and  $g'$  as the small-scale fading of the PT-BD link, the BD-PR link and the PT-PR link, respectively. Accordingly, we have  $h = h' D_{ps}^{-\alpha_{ps}}$ ,  $f = f' D_{sr}^{-\alpha_{sr}}$  and  $g = g' D_{pr}^{-\alpha_{pr}}$ , where  $\alpha_{ps}$ ,  $\alpha_{sr}$  and  $\alpha_{pr}$  are the path loss exponents of the PT-BD link, the BD-PR link and the PT-PR link, respectively. Here  $\alpha_{ps}$ ,  $\alpha_{sr}$  and  $\alpha_{pr}$  are set as 2.7, 2.7 and 3, respectively. The BD's power reflection coefficient  $\beta$  is set as 0.8.

Fig. 2 shows the PT's rate versus the transmit power of the PT under the HIs case and the ideal case. In order to illustrate the improvement of the PT's rate caused by the BD's cooperation, we compare the PT's transmit rate under the considered network (called "Cooperation" in this figure) with the PT's rate under the network without the BD (called "Non-cooperation" in this figure). For the PT's rate under the considered network, we plot the simulation results and the theoretical results, respectively, where the simulation results are obtained via Monte Carlo simulations (marked by 'o') averaged over  $1 \times 10^6$  realizations and the theoretical results are achieved based on the derived expression (16). It can be observed that the theoretical results match well with the simulation results, which demonstrates the correctness of (16). By comparisons, we can see that the PT's rate under the considered network is always higher than that without the BD's cooperation in both the HIs case and the ideal case, which verifies Theorem 1,

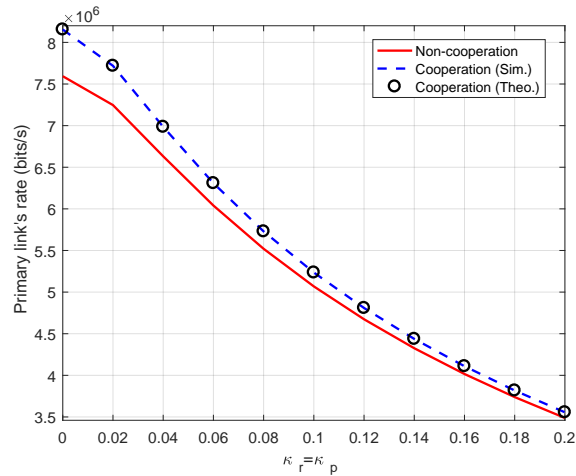


Fig. 3. The impacts of the HIs level parameters on the PT's rate.

indicating that although the HIs level has significant impacts on the PT's rate, the improvement from the BD's cooperation still exists. Besides, by comparing the rate gains under the HIs case and the ideal case, we can also find that the existence of the HIs not only reduces the achievable rate at the PT, but also degrades the rate gain.

Fig. 3 illustrates the impacts of the HIs level parameters on the PT's rate. Here we set the values of  $\kappa_r$  and  $\kappa_p$  are same and vary from 0 to 0.2. It can be observed that the simulation results with the BD's cooperation (marked by 'o') always match well with the theoretical results via (16), indicating the correctness of theoretical derivations. We can also see that the PT's rate with/without the BD's cooperation decrease when the HIs level parameters increase, since the existence of the HIs degrades the achievable rate at the PT and the larger the HIs level parameters are, the smaller the PT's rate is. Besides, the rate gain from BD's cooperation always exists no matter what the HIs level is and a larger HIs level brings a smaller rate gain.

## V. CONCLUSIONS

In this paper, we have investigated the impacts of HIs on the mutualistic cooperative AmBC network. We have proven that the rates of both primary and AmBC links decrease in the presence of HIs and that there exist rate ceilings for both the primary and AmBC links in the presence of HIs. We have validated

that the HIs do not destroy the mutualism relationship between the AmBC and primary link and have also derived closed-form rate expressions for both the primary and AmBC links under the assumption that the BD's message follows a symmetric complex Gaussian distribution. Simulation results have validated our derived results.

## APPENDIX A

Let define the following function, i.e.,  $\phi(x) = \frac{P_0 h \beta g x + P_0 f}{P_0 (h \beta g x + f) \kappa^2 + \sigma^2}$ . Taking the first derivative of  $\phi(x)$  with respect to  $x$ , we have

$$\phi'(x) = \frac{P_0^2 h \beta g \sigma^2}{(P_0 (h \beta g x + f) \kappa^2 + \sigma^2)^2} \quad (\text{A.1})$$

It is clear from (A.1) that  $\phi(x)$  increases with  $x$  at  $x \geq 0$ . Thus, we have

$$\begin{cases} \log_2 \left( 1 + \frac{P_0 h \beta g |c_s(i)|^2 + P_0 f}{P_0 (h \beta g |c_s(i)|^2 + f) \kappa^2 + \sigma^2} \right) \\ > \log_2 \left( 1 + \frac{P_0 f}{P_0 f \kappa^2 + \sigma^2} \right), \text{ if } |c_s(i)|^2 > 0, \\ \log_2 \left( 1 + \frac{P_0 h \beta g |c_s(i)|^2 + P_0 f}{P_0 (h \beta g |c_s(i)|^2 + f) \kappa^2 + \sigma^2} \right) \\ = \log_2 \left( 1 + \frac{P_0 f}{P_0 f \kappa^2 + \sigma^2} \right), \text{ if } |c_s(i)|^2 = 0. \end{cases} \quad (\text{A.2})$$

In what follows, we examine the value of  $|c_s(i)|^2$ . In modulation schemes, different values of  $c_s(i)$  are mapped to different information. If  $|c_s(i)|^2 = 0$  holds for all  $i$ , BD cannot modulate its information to the PT's signal and the achievable rate of BD equals zero. Therefore, in order to achieve the information transmission of the AmBC link,  $|c_s(i)|^2 = 0$  cannot be always satisfied for any given  $i$ . Combining this fact,  $|c_s(i)|^2 \geq 0$  and (A.2), we reach the following result, given as

$$\begin{aligned} \mathcal{C}_p &= \mathbb{E}_{c_s(i)} \left[ B_w \log_2 \left( 1 + \frac{P_0 h \beta g |c_s(i)|^2 + P_0 f}{P_0 (h \beta g |c_s(i)|^2 + f) \kappa^2 + \sigma^2} \right) \right] \\ &> \mathbb{E}_{c_s(i)} \left[ B_w \log_2 \left( 1 + \frac{P_0 f}{P_0 f \kappa^2 + \sigma^2} \right) \right] \\ &= B_w \log_2 \left( 1 + \frac{P_0 f}{P_0 f \kappa^2 + \sigma^2} \right). \end{aligned} \quad (\text{A.3})$$

Theorem 1 can be proven by (A.3) and the proof is complete.

## APPENDIX B

As  $c_s(i)$  obeys a standard symmetric complex Gaussian distribution, the distribution of  $|c_s(i)|^2$  is an exponential function with parameter one. Based on this, (7) can be rewritten as

$$\begin{aligned}
\mathcal{C}_p &= \mathbb{E}_{c_s(i)} [R_p(c_s(i))] \\
&= \int_0^\infty B_w \log_2 \left( 1 + \frac{ax + b}{a\kappa x + b\kappa + \sigma^2} \right) \exp(-x) dx \\
&= \underbrace{\int_0^\infty B_w \log_2 ((a\kappa + a)x + b + b\kappa + \sigma^2) \exp(-x) dx}_{\Delta_1} \\
&\quad - \underbrace{\int_0^\infty B_w \log_2 (a\kappa x + b\kappa + \sigma^2) \exp(-x) dx}_{\Delta_2}, \tag{B.1}
\end{aligned}$$

where  $a = P_0 h \beta g$  and  $b = P_0 f$ . Using integration by parts, we have

$$\begin{aligned}
\Delta_1 &= -B_w \log_2 (b + b\kappa + \sigma^2 + (a\kappa + a)x) \exp(-x) \Big|_0^\infty \\
&\quad + \frac{B_w (a\kappa + a)}{\ln 2} \int_0^\infty \frac{\exp(-x)}{b + b\kappa + \sigma^2 + (a\kappa + a)x} dx \\
&= B_w \log_2 (b + b\kappa + \sigma^2) + \frac{B_w}{\ln 2} \int_0^\infty \frac{e^{-x}}{\frac{b + b\kappa + \sigma^2}{a\kappa + a} + x} dx \\
&= B_w \log_2 (b + b\kappa + \sigma^2) - \frac{B_w}{\ln 2} \exp\left(\frac{b + b\kappa + \sigma^2}{a\kappa + a}\right) \\
&\quad \times \text{Ei}\left(-\frac{b + b\kappa + \sigma^2}{a\kappa + a}\right), \tag{B.2}
\end{aligned}$$

where the last equality is derived from  $\int_0^\infty \frac{\exp(-\mu x) dx}{x + \beta} = -\exp(\mu\beta) \text{Ei}(-\mu\beta)$ , as shown in eq.(3.352.4) of [19].

Similar as above,  $\Delta_2$  can be calculated as

$$\begin{aligned}
\Delta_2 &= -B_w \log_2 (a\kappa x + b\kappa + \sigma^2) e^{-x} \Big|_0^\infty + \frac{B_w}{\ln 2} \int_0^\infty \frac{e^{-x}}{a\kappa x + b\kappa + \sigma^2} dx \\
&= \begin{cases} B_w \log_2 (b\kappa + \sigma^2) + \frac{B_w}{a\kappa \ln 2} \int_0^\infty \frac{e^{-x}}{x + \frac{b\kappa + \sigma^2}{a\kappa}} dx, & \text{if } \kappa > 0 \\ B_w \log_2 (b\kappa + \sigma^2), & \text{if } \kappa = 0 \end{cases} \\
&= B_w \log_2 (b\kappa + \sigma^2) - \begin{cases} \frac{B_w}{\ln 2} \exp\left(\frac{b\kappa + \sigma^2}{a\kappa}\right) \text{Ei}\left(-\frac{b\kappa + \sigma^2}{a\kappa}\right), & \text{if } \kappa > 0 \\ 0, & \text{if } \kappa = 0 \end{cases}. \tag{B.3}
\end{aligned}$$

Substituting (B.2) and (B.3) into (B.1), we can reach (16) and the proof is complete.

## REFERENCES

- [1] C. Xu, L. Yang, and P. Zhang, "Practical backscatter communication systems for battery-free internet of things: A tutorial and survey of recent research," *IEEE Signal Process. Mag.*, vol. 35, no. 5, pp. 16–27, 2018.
- [2] Y. Ye, L. Shi, X. Chu, and G. Lu, "On the outage performance of ambient backscatter communications," *IEEE Internet Things J.*, vol. 7, no. 8, pp. 7265–7278, 2020.
- [3] Y. Ye, L. Shi, R. Qingyang Hu, and G. Lu, "Energy-efficient resource allocation for wirelessly powered backscatter communications," *IEEE Commun. Lett.*, vol. 23, no. 8, pp. 1418–1422, 2019.
- [4] V. Liu *et al.*, "Ambient backscatter: wireless communication out of thin air," in *Proc. ACM SIGCOMM*, 2013, p. 12–16.
- [5] B. Kellogg *et al.*, "Wi-Fi backscatter: Internet connectivity for RF-powered devices," in *Proc. ACM SIGCOMM*, 2014, pp. 607–618.
- [6] S. N. Daskalakis, J. Kimionis, A. Collado, G. Goussetis, M. M. Tentzeris, and A. Georgiadis, "Ambient backscatterers using fm broadcasting for low cost and low power wireless applications," *IEEE Trans. Microw. Theory Techn.*, vol. 65, no. 12, pp. 5251–5262, 2017.
- [7] C. Liu, Z. Wei, D. W. K. Ng, J. Yuan, and Y.-C. Liang, "Deep transfer learning for signal detection in ambient backscatter communications," *IEEE Trans. Wireless Commun.*, vol. 20, no. 3, pp. 1624–1638, 2021.
- [8] Y.-C. Liang, Q. Zhang, E. G. Larsson, and G. Y. Li, "Symbiotic radio: Cognitive backscattering communications for future wireless networks," *IEEE Trans. Cogn. Commun. Netw.*, vol. 6, no. 4, pp. 1242–1255, 2020.
- [9] X. Kang, Y.-C. Liang, and J. Yang, "Riding on the primary: A new spectrum sharing paradigm for wireless-powered IoT devices," in *Proc. IEEE ICC*, 2017, pp. 1–6.
- [10] R. Long, Y.-C. Liang, H. Guo, G. Yang, and R. Zhang, "Symbiotic radio: A new communication paradigm for passive internet of things," *IEEE Internet Things J.*, vol. 7, no. 2, pp. 1350–1363, 2020.
- [11] Z. Chu, W. Hao, P. Xiao, M. Khalily, and R. Tafazolli, "Resource allocations for symbiotic radio with finite blocklength backscatter link," *IEEE Internet Things J.*, vol. 7, no. 9, pp. 8192–8207, 2020.
- [12] X. Chen, H. V. Cheng, K. Shen, A. Liu, and M.-J. Zhao, "Stochastic transceiver optimization in multi-tags symbiotic radio systems," *IEEE Internet Things J.*, vol. 7, no. 9, pp. 9144–9157, 2020.
- [13] H. Yang, Y. Ye, K. Liang, and X. Chu, "Energy efficiency maximization for symbiotic radio networks with multiple backscatter devices," *IEEE Open J. Commun. Soc.*, vol. 2, pp. 1431–1444, 2021.
- [14] Z. Ding, "Harvesting devices' heterogeneous energy profiles and QoS requirements in IoT: WPT-NOMA vs BAC-NOMA," *IEEE Trans. Commun.*, vol. 69, no. 5, pp. 2837–2850, 2021.
- [15] Q. Zhang, L. Zhang, Y.-C. Liang, and P. Y. Kam, "Backscatter-NOMA: An integrated system of cellular and internet-of-things networks," in *Proc. IEEE ICC*, 2019, pp. 1–6.
- [16] S. Zhou, W. Xu, K. Wang, C. Pan, M.-S. Alouini, and A. Nallanathan, "Ergodic rate analysis of cooperative ambient backscatter communication," *IEEE Wireless Commun. Lett.*, vol. 8, no. 6, pp. 1679–1682, 2019.

- [17] Z. Liu, G. Lu, Y. Ye, and X. Chu, "System outage probability of PS-SWIPT enabled two-way AF relaying with hardware impairments," *IEEE Trans. Veh. Technol.*, vol. 69, no. 11, pp. 13 532–13 545, 2020.
- [18] X. Li, M. Zhao, M. Zeng, S. Mumtaz, V. G. Menon, Z. Ding, and O. A. Dobre, "Hardware impaired ambient backscatter NOMA systems: Reliability and security," *IEEE Trans. Commun.*, vol. 69, no. 4, pp. 2723–2736, 2021.
- [19] I. S. Gradshteyn and I. M. Ryzhik, *Table of integrals, series, and products*, 7th ed. New York, NY, USA: Academic press, 2007.